



## Article

# Effects of Coenzyme Q10 on the Biomarkers (Hydrogen, Methane, SCFA and TMA) and Composition of the Gut Microbiome in Rats

Anastasiia Yu. Ivanova <sup>1,2</sup>, Ivan V. Shirokov <sup>3</sup>, Stepan V. Toshchakov <sup>4</sup> , Aleksandra D. Kozlova <sup>4</sup>, Olga N. Obolenskaya <sup>1</sup>, Sofia S. Mariasina <sup>1,5</sup> , Vasily A. Ivlev <sup>6</sup> , Ilya B. Gartsev <sup>7</sup> and Oleg S. Medvedev <sup>1,2,\*</sup>

- <sup>1</sup> Faculty of Medicine, Lomonosov Moscow State University, Moscow 119991, Russia  
<sup>2</sup> National Medical Research Center of Cardiology of the Ministry of Health of the Russian Federation, Laboratory of Experimental Pharmacology, Moscow 121552, Russia  
<sup>3</sup> Medical and Technical Information Technologies, Bauman Moscow State Technical University, Moscow 105005, Russia  
<sup>4</sup> Center for Genome Research, National Research Center “Kurchatov Institute”, Moscow 123098, Russia  
<sup>5</sup> Institute of Functional Genomics, Moscow State University, Moscow 119991, Russia  
<sup>6</sup> Pharmacy Resource Center, Peoples Friendship University of Russia (RUDN University), Moscow 117198, Russia  
<sup>7</sup> The Institute of Artificial Intelligence of Russian Technological University MIREA, Moscow 119454, Russia  
\* Correspondence: oleg.omedvedev@gmail.com; Tel.: +7-903-745-62-08

**Abstract:** The predominant route of administration of drugs with coenzyme Q10 (CoQ10) is administration *per os*. The bioavailability of CoQ10 is about 2–3%. Prolonged use of CoQ10 to achieve pharmacological effects contributes to the creation of elevated concentrations of CoQ10 in the intestinal lumen. CoQ10 can have an effect on the gut microbiota and the levels of biomarkers it produces. CoQ10 at a dose of 30 mg/kg/day was administered *per os* to Wistar rats for 21 days. The levels of gut microbiota biomarkers (hydrogen, methane, short-chain fatty acids (SCFA), and trimethylamine (TMA)) and taxonomic composition were measured twice: before the administration of CoQ10 and at the end of the experiment. Hydrogen and methane levels were measured using the fasting lactulose breath test, fecal and blood SCFA and fecal TMA concentrations were determined by NMR, and 16S sequencing was used to analyze the taxonomic composition. Administration of CoQ10 for 21 days resulted in a 1.83-fold ( $p = 0.02$ ) increase in hydrogen concentration in the total air sample (exhaled air + flatus), a 63% ( $p = 0.02$ ) increase in the total concentration of SCFA (acetate, propionate, butyrate) in feces, a 126% increase in butyrate ( $p = 0.04$ ), a 6.56-fold ( $p = 0.03$ ) decrease in TMA levels, a 2.4-fold increase in relative abundance of *Ruminococcus* and *Lachnospiraceae AC 2044 group* by 7.5 times and a 2.8-fold decrease in relative representation of *Helicobacter*. The mechanism of antioxidant effect of orally administered CoQ10 can include modification of the taxonomic composition of the gut microbiota and increased generation of molecular hydrogen, which is antioxidant by itself. The evoked increase in the level of butyric acid can be followed by protection of the gut barrier function.

**Keywords:** coenzyme Q10; antioxidant; molecular hydrogen; short-chain fatty acids; trimethylamine; gut microbiota



**Citation:** Ivanova, A.Y.; Shirokov, I.V.; Toshchakov, S.V.; Kozlova, A.D.; Obolenskaya, O.N.; Mariasina, S.S.; Ivlev, V.A.; Gartsev, I.B.; Medvedev, O.S. Effects of Coenzyme Q10 on the Biomarkers (Hydrogen, Methane, SCFA and TMA) and Composition of the Gut Microbiome in Rats. *Pharmaceuticals* **2023**, *16*, 686. <https://doi.org/10.3390/ph16050686>

Academic Editors: Tyler W. LeBaron and Jan Slezak

Received: 20 March 2023

Revised: 21 April 2023

Accepted: 27 April 2023

Published: 2 May 2023



**Copyright:** © 2023 by the authors. Licensee MDPI, Basel, Switzerland. This article is an open access article distributed under the terms and conditions of the Creative Commons Attribution (CC BY) license (<https://creativecommons.org/licenses/by/4.0/>).

## 1. Introduction

The Coenzyme Q10 (CoQ10) was first identified by Crane et al. (1957) in the beef heart mitochondria [1]. CoQ10, located in the inner mitochondrial membrane plays a key role in the process of oxidative phosphorylation, and production of ATP, as highlighted by Nobel Prize winner of the 1978, Peter Mitchell. CoQ is composed of a benzoquinone ring and a polyisoprenoid tail containing between 6 and 10 species-specific subunits conferring stability to the molecule inside the phospholipid bilayer. The isoprene chain in *Saccharomyces cerevisiae* contains six subunits (CoQ6), seven subunits are present in

*Crucianella maritima* (CoQ7), eight in *E. coli* (CoQ8), nine and ten in mice and rats (CoQ9 and CoQ10), and ten in humans (CoQ10) [2,3]. This molecule has traditionally been used clinically as an enhancer of mitochondrial function or an antioxidant intended to either palliate or diminish the oxidative damage that may worsen the physiological outcome of a wide range of diseases (cardiovascular, endocrine etc.) [3]. The absorption of CoQ10 is slow and limited due to its hydrophobicity and large molecular weight and, therefore, high doses are needed to reach a number of rat tissues [4].

Benzoquinones are synthesized by both aerobic [5] and anaerobic bacteria [6]. The physiological role of ubiquinone in bacteria is the regulation of energy metabolism, gene expression, and prevention of oxidative stress [7]. Benzoquinone compounds have been shown to act as a growth factor for some uncultured bacteria of the gut microbiome [8].

One of the colon microbiota functions is fermentation of complex carbohydrates/fibers that cannot be absorbed in the small intestine. As a result of this process, low-molecular-weight biologically active substances are formed, including gaseous metabolites (hydrogen (H<sub>2</sub>), methane (CH<sub>4</sub>), short-chain fatty acids (SCFA) and trimethylamine (TMA). A group of Japanese scientists showed that molecular hydrogen has an antioxidant effect [9]. H<sub>2</sub> is able to bind the most aggressive reactive oxygen species—hydroxyl radical (•OH) and peroxynitrite (ONOO<sup>-</sup>), increase the expression of endogenous proteins—superoxide dismutase, catalase, glutathione peroxidase, myeloperoxidase, glutathione synthase; exhibit cytoprotective properties by regulating the Nrf2-, ARE-, PI3K/Akt-, JAK2/STAT3 signaling pathways inside the cell; reduce pro-inflammatory cytokine formation [10,11]. It has been shown that H<sub>2</sub> administration in the form of hydrogen-saturated water leads to increased formation of CoQ10 in rat heart mitochondria, increased ATP generation and suppression of oxidative stress, which is accompanied by a decrease in malonic dialdehyde (MDA) levels [12].

Increased concentrations of CoQ10 in the intestinal lumen when taken orally can create conditions for changes in the composition of the intestinal microbiota, as well as influence the production of biomarkers, which, however, has not been experimentally investigated so far. Therefore, the purpose of this work was to study the effect of oral administration of CoQ10 on both the taxonomic composition of the gut microbiota in rats and the level of such biomarkers of its enzymatic activity as hydrogen, methane, SCFA and TMA.

## 2. Results

### 2.1. Determination of Gas Metabolites of Gut Microbiota (H<sub>2</sub> and CH<sub>4</sub>)

#### 2.1.1. Determination of H<sub>2</sub> and CH<sub>4</sub> in the Rat Total Air Sample on the Regular Diet

The mean values of triplicate measurements of H<sub>2</sub> and CH<sub>4</sub> levels (0 h, 3 h, 6 h) in air samples during the day before and at the end of the experiment are presented in Table 1. CH<sub>4</sub> concentrations in the air sample on the regular diet were significantly higher than H<sub>2</sub> concentrations in all experimental groups: 7-fold in the *Control* group, 9.7-fold in the *Vehicle* group, 8-fold in the *CoQ10* group. The ratio CH<sub>4</sub>/H<sub>2</sub> at the end of the experiment increased in the *Control* group by 53.8% and decreased in the *Vehicle* and *CoQ10* groups by 23.03% and 42.06%, respectively. However, no statistically significant differences were found in either group.

**Table 1.** The level of gas biomarkers of the gut microbiota (H<sub>2</sub> and CH<sub>4</sub>) in the air sample at the beginning and at the end of the experiment in rats.

	<i>Control</i>			<i>Vehicle</i>			<i>CoQ10</i>		
	Pre	Post	<i>p</i> -Value	Pre	Post	<i>p</i> -Value	Pre	Post	<i>p</i> -Value
H <sub>2</sub> , ppm	12.8 ± 2.2	11.8 ± 2.3	0.6	9.1 ± 3.2	9.2 ± 1.3	0.4	12.3 ± 2.6	13.6 ± 3.1	0.5
CH <sub>4</sub> , ppm	88.7 ± 9.5	96.5 ± 14.6	0.6	88.3 ± 14.0	74.5 ± 12.2	0.4	99.0 ± 15.7	92.7 ± 15.5	0.8
CH <sub>4</sub> /H <sub>2</sub>	8.0 ± 1.8	12.4 ± 4.1	0.3	11.9 ± 1.9	9.2 ± 1.9	0.2	10.1 ± 2.4	5.9 ± 1.5	0.1

### 2.1.2. Determination of H<sub>2</sub> and CH<sub>4</sub> in the Rat Total Air Sample in the Lactulose Test

The metabolic activity of the gut microbiota was assessed by stimulating the enzymatic activity by administration of the artificial disaccharide lactulose (4-O-β-D-galactopyranosyl-D-fructose) in the absence of food factors. Comparison of the areas under the curves (AUC) of the dynamics of H<sub>2</sub> and CH<sub>4</sub> concentration in the total air sample after lactulose loading for a period of 8 h revealed an increase in H<sub>2</sub> generation in the CoQ10 group by 1.83 times relative to baseline and was 83.26 ± 9.17 ppm\*h ( $p = 0.02$ ). A statistically significant increase in the dynamics of CH<sub>4</sub> generation was found in the Control and Vehicle groups 2.16-fold and 1.47-fold, and was 1036 ± 215 ppm\*h ( $p = 0.01$ ) and 679.6 ± 91.4 ppm\*h ( $p = 0.04$ ), respectively, shown in Figure 1.

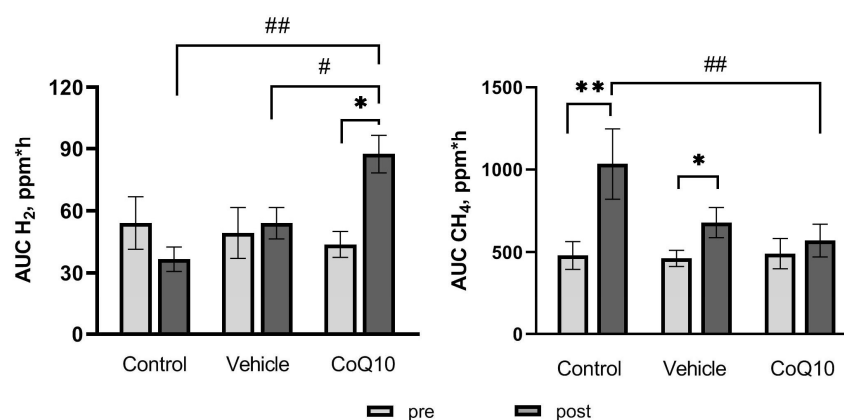


**Figure 1.** Area under the curve (AUC) of concentration of H<sub>2</sub> and CH<sub>4</sub> in rats (ppm\*h) in the lactulose test. \*  $p < 0.05$  and \*\*  $p < 0.01$ —within-group comparisons, #  $p < 0.05$  and ##  $p < 0.01$ —between-group comparisons.

### 2.2. Determination of SCFA in Plasma and Feces of Rats

In the CoQ10 group, acetic acid concentration increased at the end of the experiment by 56% ( $p = 0.04$ ), butyric acid by 126% ( $p = 0.04$ ) in the fecal samples. Total fecal SCFA concentration increased in the CoQ10 group by 63% compared to baseline values ( $p = 0.02$ ). No statistically significant differences were found in the plasma in all experimental groups. Data is presented in Table 2.

**Table 2.** The concentration of short-chain volatile fatty acids (SCFAs) in rats in the experiment. A—in feces, B—in plasma.

		Control			Vehicle			CoQ10		
		Pre	Post	<i>p</i> -Value	Pre	Post	<i>p</i> -Value	Pre	Post	<i>p</i> -Value
A.	Acetic acid, mmol/kg	5.5 ± 1.5	5.7 ± 1.2	0.8	3.9 ± 1.6	4.5 ± 1.7	0.8	4.9 ± 1.1	7.5 ± 1.8	* 0.04
	Propionic acid, mmol/kg	2.50 ± 0.81	2.62 ± 0.60	0.8	1.49 ± 0.66	1.73 ± 0.64	>0.9999	2.29 ± 0.50	3.42 ± 0.75	0.09
	Butyric acid, mmol/kg	0.44 ± 0.12	0.49 ± 0.11	0.4	0.31 ± 0.15	0.36 ± 0.13	0.7	0.28 ± 0.06	0.63 ± 0.18	* 0.04
	Total SCFA, mmol/kg	8.4 ± 2.4	8.8 ± 1.9	0.7	5.7 ± 2.4	6.6 ± 2.3	0.8	6.8 ± 1.6	11.1 ± 2.5	* 0.02
B.	Acetic acid, μmol/L	199 ± 21	215 ± 6	0.6	240 ± 19	235 ± 11	0.7	189 ± 22	246 ± 33	0.08
	Propionic acid, μmol/L	27.2 ± 6.6	23.0 ± 6.7	0.4	34.3 ± 8.1	32.1 ± 7.8	0.4	30.7 ± 9.8	36.6 ± 9.8	0.4
	Butyric acid, μmol/L	8.9 ± 1.1	7.8 ± 1.9	0.6	8.4 ± 0.7	8.8 ± 1.0	0.7	7.0 ± 0.8	7.0 ± 0.6	0.98
	Total SCFA, μmol/L	233 ± 27	244 ± 8	0.7	282 ± 25	276 ± 18	0.7	227 ± 31	290 ± 43	0.1

\*  $p < 0.05$  significant differences in the «pre-post» condition.

### 2.3. Determination of TMA in the Feces of Rats

The concentration of TMA in the feces of rats in the *CoQ10* group at the end of the experiment was  $1.12 \pm 0.44$   $\mu\text{mol/g}$  and was 6.56 times lower than the baseline level ( $p = 0.03$ ), as shown in Figure 2.

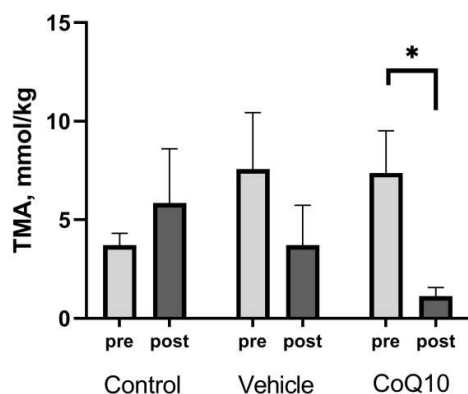


**Figure 2.** Trimethylamine (TMA) concentration in the feces of rats. \*  $p < 0.05$  significant differences in the «pre-post» condition.

### 2.4. Determination of CoQ10 in Plasma and Feces of Rats

At the end of the experiment, CoQ10 levels in the *CoQ10* group were increased 2.2 times and 5.9 times in plasma and feces, respectively, compared to than its average content in the other experimental groups ( $p < 0.01$ ) (Figure 3).

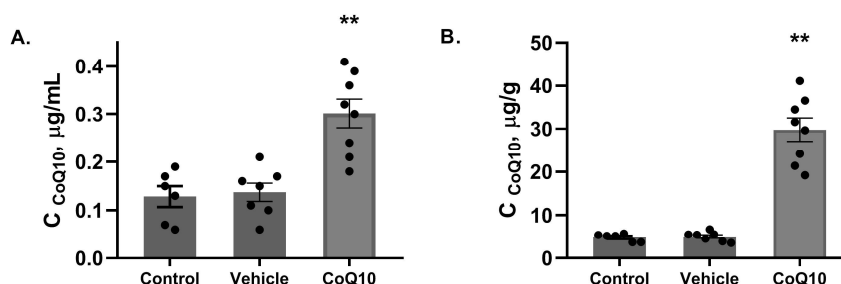


**Figure 3.** The concentration of CoQ10 in rats at the end of the experiment in plasma (A), in feces (B). \*\*  $p < 0.01$ , *CoQ10 vs. Control, Vehicle*—significant differences in the «post» condition.

### 2.5. Analysis of the Gut Microbiota Composition

13,556 amplicon sequence variants (ASVs) out of 917,866 total reads were obtained after sequencing. On average, there were about 6374 reads per replicate. After filtering, trimming and chimera removal with DADA2 R package (REF) there were obtained 1127 ASVs which was associated with 138 genera. ASV rarefaction curves built with the Vegan R package reached the saturation of approximately 1500 reads for all sequenced samples indicating the sufficiency of sequencing depth (Supplementary Figure S1).

#### 2.5.1. Alpha-Diversity Analysis

The alpha-diversity analysis performed by the microeco package was using the Shannon and Inv. Simpson indexes. Comparison made by t-test showed a significant difference in Shannon index between “pre-post” in the *Vehicle* group ( $p = 0.03$ ) and *CoQ10* group ( $p = 0.03$ ). The Inv. Simpson index increased only in the *CoQ10* group ( $p = 0.0008$ ) (Figure 4A).

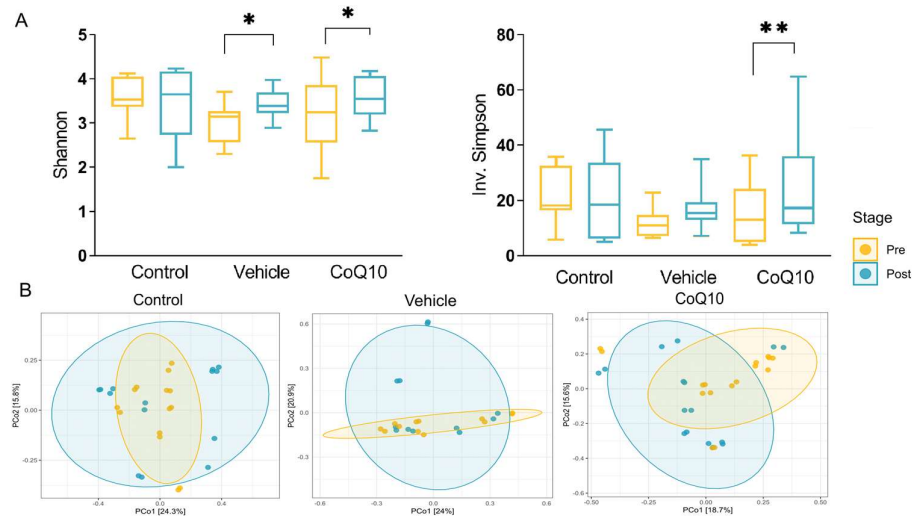


**Figure 4.** Visualization of alpha–diversity analysis of the microbiota in the «pre–post» experimental groups (A), Principal coordinate analysis (PcoA) of bacterial communities in the «pre–post» experimental groups (B). \*\*  $p < 0.01$ ; \*  $p < 0.05$  statistically significant differences in the «pre–post» condition.

Difference between microbial diversity in groups was verified with conducted a permutational multivariate analysis of variance (ADONIS, “adonis2” function) based on Euclidean dissimilarities and on the data with centroid log ratio by reason of the compositional behaviour of the absolute data (“phyloseq::distance” function). Permanova showed a significant difference in bacteria representatives in different experimental groups (betadisper  $pV > 0.01$ —variances are homogenous, adonis2  $pV = 0.001$ ). Principal coordinate analysis (PcoA) based on Bray–Curtis dissimilarities on relative normalisation revealed a significant separation of samples according to different experimental groups (Figure 4B).

### 2.5.2. Microbial Community Composition

The community composition of the gut microbiota in rats was dominated by *Firmicutes* and *Bacteroidota* phyla (Figure 5). Differential abundance at the phylum level in the pre- and post-treatment states was similar in all experimental groups. However slight decrease of *Campylobacterota* and *Desulfobacterota* was detected at the end of the experiment in all three groups (Supplementary Table S2).

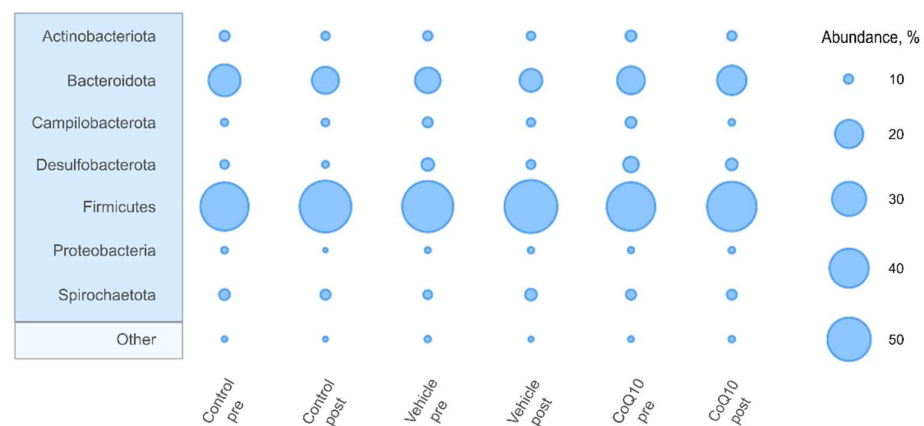


**Figure 5.** Relative abundance of top 7 phyla at pre- and post-treatment stages in all experimental groups.

It was found that in the *Control* group during the experiment, there was a significantly increase in the *F/B* ratio by 2.27 times ( $p = 0.02$ ). In the *CoQ10* group the *F/B* ratio remained unchanged (Table 3).

**Table 3.** Firmicutes/Bacteroidota ratio in the experimental groups.

	Pre	Post	<i>p</i> -Value
<i>Control</i>	2.76 ± 0.41	6.26 ± 1.46	** $p = 0.0017$
<i>Vehicle</i>	5.20 ± 1.25	8.16 ± 1.71	$p = 0.09$
<i>CoQ10</i>	4.60 ± 0.76	3.93 ± 0.64	$p = 0.25$

\*\*  $p < 0.01$  significant differences in the «pre-post» condition.

### 2.5.3. The Alterations of the Gut Microbiota

Analysis of differential abundance performed with three independent algorithms implemented in microeco package showed that abundance of 63 genera differed significantly before and after treatment at least by one method in one experimental group (Supplementary, Table, S.3). However, only 10 of these observations (3, 2 and 5 for *Control*, *Vehicle* and *CoQ10* groups, respectively) were supported by two or more algorithms and were considered for result interpretation. By this approach genera, differentially represented before and after treatment for *Control* group included *Turicibacter* (increased 10.4 times), *Erysipelatoclostridium* (increased 5.1 times), *Lachnospiraceae AC 2044 group* (decreased by 2.5 times); for *CoQ10* group included *Ruminococcus* (increased 2.4 times), *Dorea* sp. (increased from undetectable amounts to 0.36%), *Helicobacter* (decreased 2.8 times), *Lachnospiraceae AC 2044 group* (increased by 7.5 times), *Pygmaibacter* (increased from undetectable amounts to 0.15%). However, except of *Helicobacter*, which mean abundance before treatment was 2.4% and decreased to 0.6%, all of these genera were minor and represented less than 1% of the community.

### 2.5.4. Correlation Analysis between Taxonomic Composition and the Level of Metabolites of Gut Microbiota

Correlations analysis between gut microbiome and metabolic markers with following comparison of the groups showed a negative relationship with *Fecalibacterium* ( $r = -0.8131$ ,  $p = 0.0004$ ); in the *Vehicle* group with *Turicibacter* ( $r = 0.7799$ ,  $p = 0.001$ ), *Clostridium sensu stricto 1* ( $r = 0.7799$ ,  $p = 0.001$ ) in *control* group (Figure 6). A positive correlation was observed with the representation of *Erysipelatoclostridium* taxa ( $r = 0.561$ ,  $p = 0.03$ ), *Allobaculum* ( $r = 0.707$ ,  $p = 0.0062$ ) and negative with *Helicobacter* ( $r = -0.5774$ ,  $p = 0.02$ ) in the *CoQ10* group. And the level of methane in exhaled air in rats in the *CoQ10* group was negatively correlated with the abundance of the genus *Lachnospiraceae AC 2044 group* ( $r = -0.593$ ,  $p = 0.02$ ). Fecal acetate, propionate, and butyrate levels were negatively correlated with the abundance of *Turicibacter* ( $r = -0.7758$ ,  $p = 0.002$ ;  $r = -0.7104$ ,  $p = 0.003$ ;  $r = 0.84$ ,  $p = 0.0001$ ) and *Clostridium sensu stricto 1* ( $r = -0.731$ ,  $p = 0.005$ ;  $r = 0.6731$ ,  $p = 0.006$ ;  $r = -0.833$ ,  $p = 0.0002$ ). Fecal TMA levels were negatively correlated with *Allobaculum* ( $r = -0.5728$ ,  $p = 0.035$ ) in the *Control* group and *Lactobacillus* ( $r = -0.6137$ ,  $p = 0.014$ ) in the *CoQ10* group.

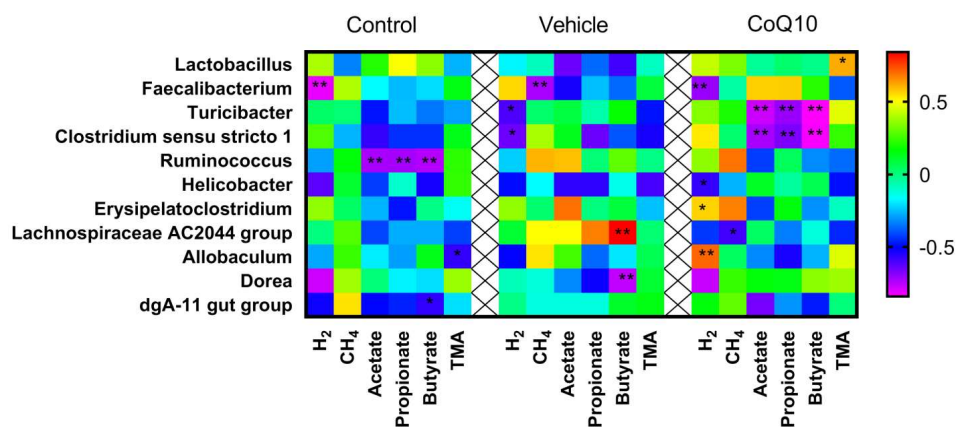


**Figure 6.** Correlation analysis between taxonomic composition and levels of gut microbiota metabolites in the experimental groups. \*\*  $p < 0.01$ ; \*  $p < 0.05$ .

### 3. Discussion

For the first time, the data have been obtained on the ability of long-term administration of CoQ10 (21 days) to increase the formation of hydrogen and SCFA by the intestinal microbiota.

Coenzyme Q (CoQ) is a redox-active quinone derivative harboring a variable number of isoprene units that range from 7 to 12 in different species. In human tissues, CoQ10 is the predominant homolog, whereas in the rodent, CoQ9 is predominant, but homologous from Q8 to Q10 were detected in rat's different tissues [13]. CoQ8 is the predominant homolog in bacteria [14,15], but in some bacteria CoQ10 is the sole respiratory quinone [16]. The possibility of the effect of injected CoQ10 on the level of CoQ8 in microbiota bacteria has not been determined in our experiments and we have not found an answer to this question in the literature. It was shown, that administration of CoQ10 in mice increase the concentration of it in the small intestine wall by 10-fold, but did not change the level of CoQ9 [17].

The reasons for greater hydrogen production during a standard fasting lactulose breath test may be: greater production of hydrogen by available species of microbiota, a relative increase in hydrogen-producing bacteria, reduced in situ hydrogen consumption in the intestinal lumen by hydrogenotrophic microorganisms, primarily methanogenic archaea and several others (e.g., *Helicobacter pylori*). No evidence is available that more H<sub>2</sub> production occurs under the influence of CoQ10 against a background of unchanged microbiota composition. However, there is still no evidence for a possible effect of CoQ10 on increasing hydrogen-producing bacteria in the microbiota. Fecal 16S rRNA sequencing revealed an increase in the proportion of *Ruminococcus* and *Lachnospiraceae* AC 2044 group bacteria, which according to literature data are involved in H<sub>2</sub> generation [18,19]. These bacterial species have [FeFe] hydrogenases required for H<sub>2</sub> generation during substrate fermentation. At the same time, administration of CoQ10 caused suppression of the relative abundance of *Helicobacter* bacteria having [NiFe] hydrogenases. According to the HydDB database [20], bacteria possessing [NiFe]-type hydrogenases are able to utilize hydrogen. The increase in the ratio of hydrogen generating/ hydrogen utilizing bacteria can explain the increased production of hydrogen by gut microbiota against the background of CoQ10 intake.

The suppression of the activity of hydrogenotrophic, methanogenic microbiota microorganisms may be of significant importance in the increase in H<sub>2</sub> formation under the influence of CoQ10. The rats used in our experiments were characterized by high content of methane in the air samples studied, and can be referred by this criterion to the group of highly methanogenic. It is known that H<sub>2</sub> formed as a result of fermentation of mainly carbohydrates is used for acetate synthesis by acetogenic bacteria, for methane synthesis by methanogenic archaea (this appears to be the main consumer of H<sub>2</sub>), and for

hydrogen sulfide synthesis by sulfate-reducing bacteria. The synthesis of one molecule of methane requires 4 molecules of hydrogen [19,21]. The increase in H<sub>2</sub> production is demonstrated occurs simultaneously with a decrease in CH<sub>4</sub> synthesis. Such explanation is supported by the recently published paper by Ruoud and colleagues [22]. The authors have showed that in cocultured of hydrogen producing *Christensenella minuta* and methane producing *Methanobrevibacter smithii* condition form flocks (very tight connections) in vitro and methanogenic *Methanobrevibacter* is able to utilise all the hydrogen produced by *Christensenella minuta*. It is unlikely that CoQ10, being a benzoquinone, directly affects the Archaea functions, since Archaea isoprenoid quinones contain Menaquinone (MK), which belongs to the naphthoquinones class [7].

The increase in the level of H<sub>2</sub> in air samples is not only a biomarker of the enzymatic activity of the intestinal microbiota, but may also have an independent significance in increasing the antioxidant defense of the body. In the work of a group of Japanese authors led by Professor Shigeo Ohta, published in 2007, it was shown that molecular hydrogen is an antioxidant that can neutralize the most active forms of oxygen—hydroxyl radical (•OH) and peroxonitrite (ONOO<sup>−</sup>) [9]. In subsequent years, more than 2000 scientific articles were published, confirming the main finding of Professor Shigeo Ohta et al. and showing the positive effect of H<sub>2</sub> introduced in the form of hydrogen saturated water as an antioxidant in ischemia/reperfusion of the brain, liver [23] and heart [24] and many other pathological conditions in the pathogenesis of which oxidative stress plays an important role [25,26]. The anti-inflammatory effects of molecular hydrogen have also been demonstrated [27,28].

Endogenous hydrogen produced by microbiota carbohydrate fermentation, is absorbed into the bloodstream and enters the liver at maximum concentration through the portal system. Nishimura and colleagues showed that the addition of a microbiota fermentation substrate (pectin) was accompanied by an increase in hydrogen production in rats. The authors found an increase in the concentration of H<sub>2</sub> in the portal vein blood (4.8-fold with a range of absolute concentrations from 4.5 to 11.5 μmol/L) and total H<sub>2</sub> output 15.5 times higher compared with controls [23].

There are reasons to compare the antioxidant effects of hydrogen and CoQ10, on models of liver ischemia/reperfusion, in the pathogenesis of damage of which oxidative stress plays a key role. In an experimental model of hepatic reperfusion ischemia in rats, it was shown that intraperitoneal injection of 10 mL/kg of hydrogen-enriched water reduced the production of proinflammatory cytokines and oxidative stress markers [29]. Administration of CoQ10 at a dose of 100 mg/kg/day for 10 days (3.3 times the dose compared to our study) also contributed to a reduction in the effects of hepatic ischemia/reperfusion [30].

In many bacteria H<sub>2</sub> generation and synthesis of short-chain fatty acids occur in parallel [31]. The increase in the partial pressure of hydrogen in the gastrointestinal tract determines thermodynamically favorable conditions for SCFA production. And the formation of acetate and butyrate is more advantageous energetically than the formation of propionate at high hydrogen concentrations in the environment [32]. This was confirmed by our study. In the *CoQ10* group an increase in the rate of hydrogen formation, recorded after the lactulose load, took place an increase the concentration of acetate by 56% ( $p = 0.04$ ) and butyrate by 126% ( $p = 0.04$ ) in the feces with respect to the initial levels.

In the *CoQ10* group, animals showed a marked inhibitory effect on the growth of *Firmicutes* bacteria. Perhaps this is related to the reduction of TMA formation in the intestine, as *Firmicutes* bacteria are characterized by the presence of genes associated with the formation of TMA [33]. The reduction of TMA levels in the intestine (precursor of TMAO) may reflect an additional positive effect of coenzyme Q10 in relation to the risk cardiovascular diseases development.

In our study, oral administration of CoQ10 at a dose of 30 mg/kg/day for 21 days resulted in increased α- and β-diversity. Increased diversity is known to rise ecosystem stability and resilience [34] and serves as a marker of gut microbiota health and metabolic capacity [35]. Comparison of changes in the relative abundance of taxa at the phylum level revealed no changes in the experimental groups *Vehicle* and *CoQ10*, while in the *Control*

group there was a marked increase in the ratio of *Firmicutes* to *Bacteroidota* phylum (*F/B*). *Firmicutes* and *Bacteroidota* are dominant phyla and a change in their ratio in the feces is considered by many researchers to be a marker of the metabolic health of the body. Increased *F/B* ratio is a sign of microbiota dysbiosis accompanying the development of such diseases as obesity, type 2 diabetes, arterial hypertension etc. Animals receiving CoQ10 showed a restrained increase in this index in our study. The positive effect of CoQ10 on the intestinal microbiota is consistent with the results of Bodkin [36], who showed that administration of CoQ10 reduced the degree of dysbiosis, prevented an increase in permeability of the intestinal wall and induced growth of “beneficial” lactobacilli in a model of hypoxia in newborn rats. CoQ10 in control rats produced the highest abundance of *Lactobacillus* species (95.3%), but this declined to 60.4% in rats with intermittent hypoxia. Low abundance phyla in CoQ10 in rats with intermittent hypoxia were *Firmicutes*, *Proteobacteria*, *Verrucomicrobia* and 2.8% unidentified organisms.

Several scientific papers confirm the effects of CoQ10 on the GI tract. An experimental model of ulcerative colitis showed antioxidant and anti-inflammatory effects of CoQ10 at a dose of 30 mg/kg by increasing the content of glutathione, catalase activity, reduced malonic dialdehyde level in the colon tissues [37]. Coenzyme Q was found to accumulate well in the intestinal walls throughout the intestine during radiation exposure in mice and protect the crypts from peroxidation and apoptosis [17]. Possibly, the increased activity of enzymatic antioxidants against the background of CoQ10 application may be partially related to the formation of endogenous hydrogen by the gut microbiota.

In the literature, there are indications of the ability of molecular hydrogen to enhance the effects of CoQ10 at the mitochondrial level. In the study of Gvozdjaková [12] the administration of hydrogen-saturated water *per os* on the second day led to the stimulation of mitochondrial respiratory electron chain function in rat cardiomyocytes, increased the level and rate of ATP production by Complex I and Complex II substrates, as well as to an increase in coenzyme Q formation in mitochondria. Combining results of our study with the results of Gvozdjaková we propose a hypothesis on the existence of positive feedback for the antioxidant effects of CoQ10.

An increase in the intestine concentration of orally administered CoQ10 is followed by the changes in composition of microbiota and increase in hydrogen production. The more of hydrogen are absorbed into the blood, reaches mitochondria of the different organ and tissues and facilitates production of ATP and antioxidant activity of CoQ10.

## 4. Materials and Methods

### 4.1. Animals and Experimental Design

All experimental procedures were carried out according to the Guide of the Care and Use of Laboratory Animals (8th edition) and other approved guidelines. The research protocol was approved by the Bioethics Commission of Moscow State University, Institute of Biology (Protocol 129-a, 12 May 2021).

The study was performed on 22 male Wistar rats (210–230 g), which were purchased from the nursery of laboratory animals branch “Stolbovaya”, Scientific Center for Biomedical Technologies of the Federal Medical and Biological Agency of Russia (Stolbovaya, Russia). The rats were kept under 12 h light/dark conditions with free access to water and food, humidity and temperature control was also performed. The adaptation period after transportation was at least 14 days.

The animals were randomized into three groups.

Group 1—*Control* (n = 6)—purified water intake;

Group 2—*Vehicle* (n = 8)—solvent of the coenzyme Q10;

Group 3—*CoQ10* (n = 8)—coenzyme Q10 30 mg/kg/day.

All rats consumed a chow diet for laboratory animals without any restriction. The substances were applied intragastrically in rats daily for 21 days. Group 3 rats received coenzyme Q10 as part of “Kudesan forte”, *vehicle* (group 2) and purified water (group 1) were administered in an equivalent volume (not more than 1 mL). The same dose

of coenzyme Q10 (30 mg/kg/day) was used in Ewees' work [37]. The group *Vehicle* was introduced additionally due to the possible modulating effect of excipients on the intestinal microbiota.

Composition of "Kudesan Forte", Rusfik LLC, Recordati S.p.A., Italy (1 mL): coenzyme Q10 60 mg, vitamin E 6.8 mg, purified water, macrogol glyceryl hydroxystearate, sodium benzoate, citric acid, ascorbyl palmitate.

The taxonomic composition of the gut microbiota, the level of H<sub>2</sub>, CH<sub>4</sub> in the air sampling, the level of SCFAs in plasma and feces, and TMA in rat's feces were evaluated at the beginning and end of the experiment.

#### 4.2. Determination of Gas Metabolites of Gut Microbiota (H<sub>2</sub> and CH<sub>4</sub>)

The metabolic activity of the gut microbiota was assessed by measuring the concentration of gaseous metabolites of the microbiota (H<sub>2</sub> and CH<sub>4</sub>) in the total air sample (exhaled air + flatus). Measurements for each rat were performed in two stages:

##### 4.2.1. Determination of H<sub>2</sub> and CH<sub>4</sub> in the Rat Total Air Sample on the Regular Diet

Air sampling was performed at three time points (0 h, 3 h, 6 h) in rats without restricted access to water and food starting at 10:00 am. At the end of the measurements, the animals were seated in metabolic chambers for 12 h of fasting with free access to water. The next day, measurements were taken in the lactulose test.

##### 4.2.2. Determination of H<sub>2</sub> and CH<sub>4</sub> in the Rat Total Air Sample in the Lactulose Test

Air sampling was performed at 7 time points (0, 2, 4, 5, 6, 7, 8 h). The first measurement was performed on an empty stomach. Then, an aqueous solution of lactulose (FreseniusKabi IPSUM S.r.l., Vicchio, Italy) was administered intragastrically at a dose of 2.0 g/kg of rat weight. Then the rats were placed in individual cages until the next time point. Next, a lactulose-evoked concentration-time curve was plotted for H<sub>2</sub> and CH<sub>4</sub>, and the area under the AUC<sub>0-8 h</sub> curve (ppm\*h) was calculated, which reflects the rate of gas generation during 8 h of measurements.

At the end of 21 day of the experiment, both steps of gas metabolite determination were repeated sequentially.

#### 4.3. Experimental Setup for Sampling Total Air Samples of Rats

To accumulate hydrogen and methane released by the rat (exhaled air + flatus), an installation was designed in our modification, similar to the one presented in the work of Gumbman [38] (Figure 7).

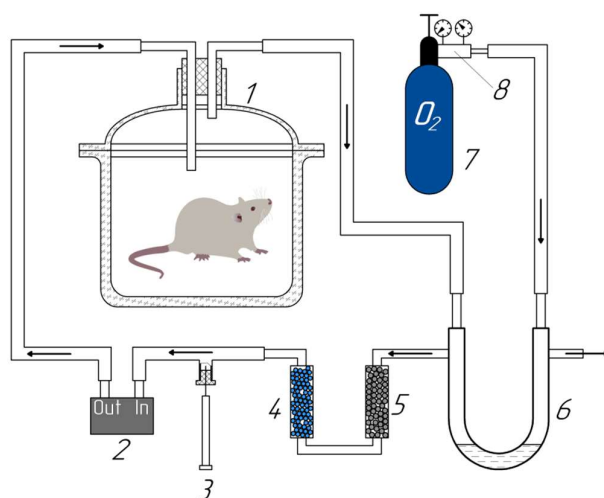


**Figure 7.** Diagram of the experimental setup for collecting the total air sample in the experiment. 1—desiccator, 2—air pump, 3—glass syringe, 4—moisture absorbent (hydrogel), 5—carbon dioxide absorbent (soda lime), 6—manometer, 7—oxygen cylinder, 8—gas pressure reducer.

The installation consisted of a glass desiccator with a volume of 1.8 L and a life support system. Two cartridges were sequentially built into the air recirculation system, one of which was filled with sodium lime to remove CO<sub>2</sub>, the second with hydrogel to absorb water condensate formed during the animal's respiration. A U-shaped manometer filled with mineral oil was used to supply oxygen to the system. When O<sub>2</sub> was consumed by the rat, the air pressure in the recirculation system decreased and then oxygen entered the system through a U-shaped pressure manometer. This ensured the oxygen concentration at the level of 19–22%, sufficient to ensure the vital functions of the animal. The time during which the rat was in the air recirculation system was calculated from the free volume of the desiccator and the rat's air exchange rate from tabular values ( $27.27 \pm 2.39$  mL/min \* 100 g) [39]. Air circulation and oxygen content control were provided by a device built at the Saint Petersburg State University of Aerospace Instrumentation (SUAI, St. Petersburg, Russia) and consisting of a pump and an oxygen sensor (OKSIK-3, Russia) for monitoring the oxygen level in the system. This device provides an air flow at the 400 mL/min rate and estimates the oxygen concentration in the flow in the range of 0–100% with a resolution of 0.1%. Supply and exhaust ventilation were provided through 2 stainless steel tubes inserted into the rubber stopper of the desiccator.

After holding the rat in the desiccator for an estimated time, an air sample in the volume of 1 mL was taken with a Hamilton gas-tight glass syringe through a valve built into the recirculation tube system.

#### 4.4. Measurement of H<sub>2</sub> and CH<sub>4</sub> Concentrations in the Total Air Sample

The concentration of H<sub>2</sub> and CH<sub>4</sub> in the air sample was measured by gas chromatography (TRILyzer mBA-3000, Taiyo Instruments Inc., Japan). As a carrier gas, we used artificial air gas of "A" quality (TU 6-21-5-82): oxygen (O<sub>2</sub>) (20.9%) + nitrogen (N<sub>2</sub>) (the rest). The measurements were carried out at a carrier gas flow rate in the chromatograph system of 30 mL/min and a column temperature of 50 °C. Gas air mixtures with 5 ppm (low point) and 50 ppm (high point) volume concentrations of H<sub>2</sub> and CH<sub>4</sub> were used to calibrate the gas chromatograph. Before starting measurements of animal samples, the background values of H<sub>2</sub> and CH<sub>4</sub> concentrations in the ambient air were measured. Background values were subtracted from the values obtained from the analysis of the total air sample from the animal.

#### 4.5. Collection of Fecal and Plasma Samples

Fecal and blood samples were taken twice: at the beginning and at the end of the experiment. Fecal samples were collected in individual Eppendorf-type tubes, quickly frozen in liquid nitrogen and stored at  $-70\text{ }^{\circ}\text{C}$  until analysis. For sequencing, fecal samples were taken and stored at  $-70\text{ }^{\circ}\text{C}$  until analysis without prior freezing in liquid nitrogen.

Blood sampling was performed from the sublingual vein after preanesthesia of the animal with isoflurane using Pureline M6000 inhalation anesthesia machine (Supera Anesthesia Innovations, Estacada, OR, USA). Blood samples of 1 mL were collected in Eppendorf-type tubes with heparin. Samples were then centrifuged at  $5000\times g$  for 3 min. 0.3–0.5 mL of plasma was collected, frozen, and stored at  $-70\text{ }^{\circ}\text{C}$  until further analysis.

#### 4.6. Quantification of SCFA in Rat Feces and Blood

Quantification of rat feces and blood SCFA was performed by nuclear magnetic resonance (NMR) spectroscopy.

##### 4.6.1. Fecal Sample Preparation

Sample of fecal matter (0.1–0.5 g) was mixed with  $1\times$  PBS buffer (Amresco, OH, USA) in a ratio of 1:3 and homogenized using a PrecellysEvolution homogenizer (Bertin Technologies, Montigny-le-Bretonneux, France) in tubes containing zirconium oxide beads (3 times for 10 s). After that it was placed on an orbital shaker for 30 min and centrifuged at  $16,000\times g$  for 15 min at  $4\text{ }^{\circ}\text{C}$ .

The supernatant was filtered through Amiconultracellulose cartridges with a cut-off molecular weight of 10 kDa (Merck Millipore, NJ, USA). The filtrate was dried in a vacuum concentrator (Eppendorf Concentrator plus™) for 3 h until the solvent completely evaporated, and then it was freeze-dried using FreeZone 2.5 freeze dry system (Labconco, Kansas City, MO, USA) for 3 h and kept at  $-60\text{ }^{\circ}\text{C}$  until measurements.

##### 4.6.2. Blood Plasma Sample Preparation

Blood plasma samples were prepared according to the recommendations [40]. 200  $\mu\text{L}$  of blood plasma was mixed with methanol (200  $\mu\text{L}$ ) and chloroform (200  $\mu\text{L}$ ), precooled to  $-20\text{ }^{\circ}\text{C}$ . The samples were thoroughly vortexed, kept for 10 min at  $5\text{ }^{\circ}\text{C}$ , and then centrifuged at  $16,000\times g$  for 30 min at  $5\text{ }^{\circ}\text{C}$ . The upper water-methanol layer was carefully separated and dried on a vacuum concentrator (Eppendorf Concentrator plus™) for 6 h until the solvent completely evaporated, and then freeze-dried using FreeZone 2.5 freeze dry system (Labconco, Kansas City, MO, USA) for 3 h and stored at  $-60\text{ }^{\circ}\text{C}$  until measurements.

##### 4.6.3. NMR Spectra Measurements

The dried extracts were dissolved in 550  $\mu\text{L}$  of deuterated phosphate buffer (20 mM, pH 8.0) containing sodium azide (2 mM) as a preservative against bacteria and DSS-d6 (0.1 mM) as an internal standard. After centrifugation (10 min, room temperature) samples were placed into standard 5 mm NMR tubes. The spectra were acquired on AVANCE Neo 700 MHz NMR spectrometer (Bruker BioSpin, Reinstetten, Germany) equipped with a Prodigy triple resonance cryoprobe (Bruker, Reinstetten, Germany). The spectra were acquired at  $25\text{ }^{\circ}\text{C}$  using the noesypr1d pulse sequence with the following parameters: 131,072 data points, 4 dummy scans, 400 scans for fecal and 600 for plasma samples, 19.8364 ppm spectral width; 4.7 s accumulation time, 6.0 s relaxation delay between scans.

##### 4.6.4. Identification and Quantification of Metabolites

Spectra processing and metabolite identification were performed in the Chenomx v9 (Chenomx Inc., Edmonton, AB, Canada) program based on the built-in database, as well as the Human Metabolome Database [41]. The assignments were confirmed by adding reference SCFA compounds. The concentrations of metabolites were measured related to DSS peak area in Chenomx v9 (Chenomx Inc., Edmonton, AB, Canada).

#### 4.7. HPLC Analysis

The fecal samples were homogenized in 96% C<sub>2</sub>H<sub>5</sub>OH (ratio 1:4) by ultrasound homogenizer. 100 µL homogenate was transferred in an individual eppendorf-type tube for further extraction. N-Hexan (250 µL) was added to the fecal samples, ethanol (200 µL) and n-hexane (500 µL) were added to 100 µL of plasma and were shaken for 10 min, then centrifuged at 5000 × g for 5 min. The upper hexan layer was collected and the extraction was repeated. The total extract amount was evaporated and dissolved in 100 µL of 96% ethanol. CoQ10 levels were measured using high-performance liquid chromatography with electrochemical detection (Environmental Sciences Associate, Inc., Chelmsford, MA, USA): model 580 pump and electrochemical detector “Coulchem II”, in isocratic mode on Luna column 150 × 4.6 mm with sorbent C18 (5 µm) at a flow rate of the eluent of 1.3 mL/min. The mobile phase was 0.3% of NaCl in the mixture ethanol-methanol-7% HClO<sub>4</sub> (970:20:10). Electrochemical detection carried out the oxidizing mode using an analytical cell (model 5011) with the voltage of −50 mV and +350 mV applied for the two pairs of electrodes, correspondingly. Chromatographic data registration and processing carried out by using of the Environmental Sciences Associate Inc software (Chelmsford, MA, USA). The extract was analyzed both before and after the complete recovery of ubiquinol (by adding the solution of sodium tetrahydroborate in ethanol).

#### 4.8. Analysis of Microbial Community Composition

##### 4.8.1. DNA Extraction and High-Throughput 16S Sequencing

Extraction of DNA from feces was performed with QIAampPowerFecal Pro DNA Kit (Qiagen, Hilden, Germany), according to manufacturer’s instructions. Quantity of DNA was assessed using Qubit™ 4 fluorometer (Thermo Fisher Scientific, MA, USA). 1–2 ng of DNA was used for library preparation.

Libraries of 16S rRNA V4 hypervariable region were prepared using a two-step PCR strategy as described earlier [42]. Two library replicates were prepared for each sample. The first round of PCR was performed using qPCRmix-HS SYBR (Evrogen, Moscow, Russia) with the following primers at a concentration of 0.25 µM: V4\_515F TCGTCGGCAGCAGCGTCAGATGTGTGTGATAAGAGACAG [NN] GTGBCAGCMGC-CGCGGTAA and V4\_805R GTCTCTCGTGGTGGCTCGGAGATGTGTGTAGATAAGACAG [NN] GACTACNVGGGTMTCTAATCC, where the first part corresponded to a partial Illumina TruSeq adapter, [NN] corresponds to 1–3 nt spacer of degenerate heterogeneity, and the last part corresponds to primers 515F [43] and Pro-mod-805R [44], respectively. After first step diluted amplification mixture was used as a matrix for the second PCR. The second PCR was performed using ScreenMix-HS (Evrogen, Moscow, Russia) using the following primers at a concentration of 0.5 µM: R1TM AATGATACACGGCGACCACCGA-GATCTACACAXXXXXXCGTCGGCAGCGTC and R2TM CAAGCAGAAGACGGCATA-CAGATXXXXXGTCTCTCGTGGTGGCTCGG, where the first part corresponded to P5 or P7 Illumina oligonucleotides, XXXXXX corresponded to 6-nt index sequences, and the last part corresponded to Illumina TruSeq partial adaptors annealing to the tail of the first PCR primers. Amplification was performed on a Veriti thermal cycler (Applied Biosystems, MA, USA). The resulting libraries were checked on an agarose gel and pooled equimolarly. The final pool was purified using the QIAquick Gel Extraction Kit (Qiagen, Germany) according to the manufacturer’s protocols.

##### 4.8.2. Primary Analysis of Sequencing Data

Sequencing was performed using the MiSeq™ Personal Sequencing System (Illumina, San Diego, CA, USA) with 2 × 156 bp paired end. The ‘Trim reads’ tool in CLC Genomics Workbench 20.0 (Qiagen, Hilden, Germany) was used to efficiently filter out and remove nucleotides corresponding to primers 515F and Pro-mod-805R. Demultiplexing was performed using the deML package [45], using zero available mismatches option. Then, read pairs were processed with DADA2 pipeline [46], according to published.

#### 4.8.3. Bioinformatics

High quality read pairs were processed with DADA2 pipeline [44], according to published protocol [46]. Taxonomy of amplified sequence variants (ASVs) was determined with naive Bayesian classifier using the Silva138 database [47]. For further analysis reads were rarefied using the phyloseq package [48]. The obtained ASV reference sequences, sample metadata, abundance tables, and taxonomy were imported into the phyloseq package, and all further operations were performed with the phyloseq object. Community differences in each group were assessed using the *adonis* and *betadisper* functions of *vegan* package [49]. Analysis of differentially abundant genera was performed with ANCOM-BC [50], DESeq2 [51] algorithms and the Wilcoxon rank sum test, implemented in *microeco* package (multivariate analysis of variance using distance matrices) [52]. Analysis of variance was performed using the *betadisper* function.

#### 4.9. Statistical Analysis

Statistical analysis of the results was performed using GraphPadPrism 8 software (GraphPad, San Diego, CA, USA). The normality of the distribution was checked using the Shapiro-Wilk test to compare the mean values of a single index in more than two samples; for pairwise comparison of groups, the paired and unpaired t-test for dependent and independent samples was used, respectively. For pairwise comparisons of groups with non-normal distributions, the Wilcoxon test was used for dependent samples and the Mann-Whitney test for independent samples. Correlations were calculated using Pearson rank correlation coefficient. Exclusion of statistical outliers was performed using ROUT criterion with Q not exceeding 1%. Differences were considered statistically significant at  $p < 0.05$ . All data are presented as mean  $\pm$  standard error of the mean (Mean  $\pm$  SEM).

**Supplementary Materials:** The following supporting information can be downloaded at: <https://www.mdpi.com/article/10.3390/ph16050686/s1>, Figure S1: Rarefaction curves; Table S1: Relative abundance of top phyla at pre- and post-treatment stages in all experimental groups; Table S2: Analysis of differential abundance at genera level.

**Author Contributions:** Conceptualization, O.S.M.; methodology, A.Y.I., I.V.S., S.V.T., O.N.O., S.S.M. and O.S.M.; validation, A.Y.I., I.V.S., S.V.T., O.N.O. and S.S.M.; formal analysis, A.Y.I., I.V.S., S.V.T., O.N.O. and S.S.M.; investigation, A.Y.I., I.V.S., S.V.T., O.N.O., S.S.M., V.A.I. and I.B.G.; statistical assessments, A.Y.I., S.V.T. and I.B.G.; writing-original draft preparation, A.Y.I., I.V.S., S.V.T., A.D.K., S.S.M. and I.B.G.; writing-review and editing, A.Y.I. and O.S.M.; visualization, A.Y.I., I.V.S., S.V.T. and A.D.K.; supervision, O.S.M.; project administration and funding acquisition I.B.G. and O.S.M. All authors have read and agreed to the published version of the manuscript.

**Funding:** The Russian Science Foundation (grant number 22-13-00111) supported this study. NMR metabolomics experiments were supported by the Russian Science Foundation (grant number 19-14-00115). The authors are grateful to Laboratory for magnetic Tomography and spectroscopy of the Moscow State University (Moscow, Russia) and to Pharmacy Resource Center of RUDN University (Moscow, Russia) for the opportunity to use their NMR facilities. The authors are grateful to Interdisciplinary Scientific and Educational School of Moscow University "Molecular Technologies of Living Systems and Synthetic Biology" for financial support. Bioinformatic analysis of microbial communities was supported by NRC "Kurchatov Institute" according to the order #90 from 20.01.2023.

**Institutional Review Board Statement:** The research protocol (Protocol 129-a, 12 May 2021) was approved by the Bioethics Commission of Moscow State University, Institute of Biology (Moscow, Russia).

**Informed Consent Statement:** Not applicable.

**Data Availability Statement:** The data presented in this study is contained within the article. Individual values are available from the corresponding authors upon reasonable request.

**Acknowledgments:** The authors are grateful to V.A. Kilimnik (SUAI, St. Petersburg, Russia) for manufacturing and providing us with a device to measure the concentration of O<sub>2</sub> and CO<sub>2</sub> in the experimental setup.

**Conflicts of Interest:** The authors declare no conflict of interest. The funders had no role in the design of the study; in the collection, analyses, or interpretation of data; in the writing of the manuscript, or in the decision to publish the results.

## References

1. Crane, F.L.; Hatefi, Y.; Lester, R.L.; Widmer, C. Isolation of a Quinone from Beef Heart Mitochondria. *Biochim. Biophys. Acta* **1957**, *25*, 220–221. [[CrossRef](#)] [[PubMed](#)]
2. Hernández-Camacho, J.D.; Bernier, M.; López-Lluch, G.; Navas, P. Coenzyme Q10 Supplementation in Aging and Disease. *Front. Physiol.* **2018**, *9*, 44. [[CrossRef](#)] [[PubMed](#)]
3. Pastor-Maldonado, C.J.; Suárez-Rivero, J.M.; Povea-Cabello, S.; Álvarez-Córdoba, M.; Villalón-García, I.; Munuera-Cabeza, M.; Suárez-Carrillo, A.; Talaverón-Rey, M.; Sánchez-Alcázar, J.A. Coenzyme Q10: Novel Formulations and Medical Trends. *Int. J. Mol. Sci.* **2020**, *21*, 8432. [[CrossRef](#)] [[PubMed](#)]
4. Bhagavan, H.N.; Chopra, R.K. Plasma Coenzyme Q10 Response to Oral Ingestion of Coenzyme Q10 Formulations. *Mitochondrion* **2007**, *7*, S78–S88. [[CrossRef](#)]
5. Aussel, L.; Pierrel, F.; Loiseau, L.; Lombard, M.; Fontecave, M.; Barras, F. Biosynthesis and Physiology of Coenzyme Q in Bacteria. *Biochim. Biophys. Acta-Bioenerg.* **2014**, *1837*, 1004–1011. [[CrossRef](#)]
6. Ito, T.; Gallegos, R.; Matano, L.M.; Butler, N.L.; Hantman, N.; Kaili, M.; Coyne, M.J.; Comstock, L.E.; Malamy, M.H.; Barquera, B. Genetic and Biochemical Analysis of Anaerobic Respiration in *Bacteroides Fragilis* and Its Importance In Vivo. *mBio* **2020**, *11*, e03238-19. [[CrossRef](#)]
7. Abby, S.S.; Kazemzadeh, K.; Vragniau, C.; Pelosi, L.; Pierrel, F. Advances in Bacterial Pathways for the Biosynthesis of Ubiquinone. *Biochim. Biophys. Acta-Bioenerg.* **2020**, *1861*, 148259. [[CrossRef](#)]
8. Fenn, K.; Strandwitz, P.; Stewart, E.J.; Dimise, E.; Rubin, S.; Gurubacharya, S.; Clardy, J.; Lewis, K. Quinones Are Growth Factors for the Human Gut Microbiota. *Microbiome* **2017**, *5*, 161. [[CrossRef](#)]
9. Ohsawa, I.; Ishikawa, M.; Takahashi, K.; Watanabe, M.; Nishimaki, K.; Yamagata, K.; Katsura, K.I.; Katayama, Y.; Asoh, S.; Ohta, S. Hydrogen Acts as a Therapeutic Antioxidant by Selectively Reducing Cytotoxic Oxygen Radicals. *Nat. Med.* **2007**, *13*, 688–694. [[CrossRef](#)]
10. Barancik, M.; Kura, B.; Lebaron, T.W.; Bolli, R.; Buday, J.; Slezak, J. Molecular and Cellular Mechanisms Associated with Effects of Molecular Hydrogen in Cardiovascular and Central Nervous Systems. *Antioxidants* **2020**, *9*, 1281. [[CrossRef](#)]
11. Ohta, S. Direct Targets and Subsequent Pathways for Molecular Hydrogen to Exert Multiple Functions: Focusing on Interventions in Radical Reactions. *Curr. Pharm. Des.* **2020**, *27*, 595–609. [[CrossRef](#)]
12. Gvozdjaková, A.; Kucharská, J.; Kura, B.; Vančová, O.; Rausová, Z.; Sumbalová, Z.; Uličná, O.; Slezák, J. A New Insight into the Molecular Hydrogen Effect on Coenzyme Q and Mitochondrial Function of Rats. *Can. J. Physiol. Pharmacol.* **2020**, *98*, 29–34. [[CrossRef](#)]
13. Battino, M.; Francisco, J.; Huertas, R.; Genova, M.L.; Lenaz, G.; Marchetti, M. Natural distribution and occurrence of coenzyme Q homologues. *Membr. Biochem.* **1990**, *9*, 179–190. [[CrossRef](#)]
14. Collins, M.D.; Jones, D. Distribution of Isoprenoid Quinone Structural Types in Bacteria and Their Taxonomic Implication. *Microbiol. Rev.* **1981**, *45*, 316–354. [[CrossRef](#)]
15. Nowicka, B.; Kruk, J. Occurrence, Biosynthesis and Function of Isoprenoid Quinones. *Biochim. Biophys. Acta-Bioenerg.* **2010**, *1797*, 1587–1605. [[CrossRef](#)]
16. Li, C.M.; Wang, X.P.; Zhou, L.Y.; Chen, G.J.; Du, Z.J. *Pelagivirga dicentrarchi* Sp. Nov., a Member of the Family *Rhodobacteraceae* Isolated from the Gut Microflora of Sea Bass (*Dicentrarchus labrax* L.). *Antonie van Leeuwenhoek. Int. J. Gen. Mol. Microbiol.* **2020**, *113*, 293–301. [[CrossRef](#)]
17. Shimizu, Y.; Mukumoto, N.; Idrus, N.; Akasaka, H.; Inubushi, S.; Yoshida, K.; Miyawaki, D.; Ishihara, T.; Okamoto, Y.; Yasuda, T.; et al. Amelioration of Radiation Enteropathy by Dietary Supplementation With Reduced Coenzyme Q10. *Adv. Radiat. Oncol.* **2019**, *4*, 237–245. [[CrossRef](#)]
18. Benoit, S.L.; Maier, R.J.; Sawers, R.G.; Greening, C. Molecular Hydrogen Metabolism: A Widespread Trait of Pathogenic Bacteria and Protists. *Microbiol. Mol. Biol. Rev.* **2020**, *84*, e00092-19. [[CrossRef](#)]
19. Medvedev, O.S. Role of Human and Animal Microbiome's Hydrogen and Methane in an Antioxidant Organism Defense. *UspekhiSovremennoiBiologii* **2022**, *142*, 349–364. (In Russian)
20. Søndergaard, D.; Pedersen, C.N.S.; Greening, C. HydDB: A Web Tool for Hydrogenase Classification and Analysis. *Sci. Rep.* **2016**, *6*, 34212. [[CrossRef](#)]
21. Krajmalnik-Brown, R.; Ilhan, Z.E.; Kang, D.W.; DiBaise, J.K. Effects of Gut Microbes on Nutrient Absorption and Energy Regulation. *Nutr. Clin. Pract.* **2012**, *27*, 201–214. [[CrossRef](#)] [[PubMed](#)]
22. Ruaud, A.; Esquivel-Elizondo, S.; de la Cuesta-Zuluaga, J.; Waters, J.L.; Angenent, L.T.; Youngblut, N.D.; Ley, R.E. Syntrophy via Interspecies H<sub>2</sub> Transfer between *Christensenella* and *Methanobrevibacter* Underlies Their Global Cooccurrence in the Human Gut. *mBio* **2020**, *11*, e03235-19. [[CrossRef](#)] [[PubMed](#)]
23. Nishimura, N.; Tanabe, H.; Sasaki, Y.; Makita, Y.; Ohata, M.; Yokoyama, S.; Asano, M.; Yamamoto, T.; Kiriya, S. Pectin and High-Amylose Maize Starch Increase Caecal Hydrogen Production and Relieve Hepatic Ischaemia-Reperfusion Injury in Rats. *Br. J. Nutr.* **2012**, *107*, 485–492. [[CrossRef](#)] [[PubMed](#)]

24. Nie, C.; Ding, X.; Rong, A.; Zheng, M.; Li, Z.; Pan, S.; Yang, W. Hydrogen Gas Inhalation Alleviates Myocardial Ischemia-Reperfusion Injury by the Inhibition of Oxidative Stress and NLRP3-Mediated Pyroptosis in Rats. *Life Sci.* **2021**, *272*, 119248. [[CrossRef](#)]
25. Yang, M.; Dong, Y.; He, Q.; Zhu, P.; Zhuang, Q.; Shen, J.; Zhang, X.; Zhao, M. Hydrogen: A Novel Option in Human Disease Treatment. *Oxid. Med. Cell. Longev.* **2020**, 1–17. [[CrossRef](#)]
26. Gebreyesus Abisso, T.; Mawulikplimi Adzavon, Y.; Zhao, P.; Zhang, X.; Zhang, X.; Liu, M.; Wang, L.; Ma, X.; Zhen, W. Current Progress in Molecular Hydrogen Medication: Protective and Therapeutic Uses of Hydrogen against Different Disease Scenarios. *Intern. Med.* **2020**, *10*, 1. [[CrossRef](#)]
27. Zhou, G.; Goshi, E.; He, Q. Micro/Nanomaterials-augmented Hydrogen Therapy. *Adv. Healthc. Mater.* **2019**, *8*, 1900463. [[CrossRef](#)]
28. Chen, S.; Zhu, Y.; Xu, Q.; Jiang, Q.; Chen, D.; Chen, T.; Xu, X.; Jin, Z.; He, Q. Photocatalytic Glucose Depletion and Hydrogen Generation for Diabetic Wound Healing. *Nat. Commun.* **2022**, *13*, 5684. [[CrossRef](#)]
29. Liu, Y.; Yang, L.; Tao, K.; Vizcaychipi, M.P.; Lloyd, D.M.; Sun, X.; Irwin, M.G.; Ma, D.; Yu, W. Protective Effects of Hydrogen Enriched Saline on Liver Ischemia Reperfusion Injury by Reducing Oxidative Stress and HMGB1 Release. *BMC Gastroenterol.* **2014**, *14*, 1–9. [[CrossRef](#)]
30. Mahmoud, A.R.; Ali, F.E.M.; Abd-Elhamid, T.H.; Hassanein, E.H.M. Coenzyme Q10 Protects Hepatocytes from Ischemia Reperfusion-Induced Apoptosis and Oxidative Stress via Regulation of Bax/Bcl-2/PUMA and Nrf-2/FOXO-3/Sirt-1 Signaling Pathways. *Tissue Cell* **2019**, *60*, 1–13. [[CrossRef](#)]
31. Carbonero, F.; Benefiel, A.C.; Gaskins, H.R. Contributions of the Microbial Hydrogen Economy to Colonic Homeostasis. *Nat. Rev. Gastroenterol. Hepatol.* **2012**, *9*, 504–518. [[CrossRef](#)] [[PubMed](#)]
32. Janssen, P.H. Influence of Hydrogen on Rumen Methane Formation and Fermentation Balances through Microbial Growth Kinetics and Fermentation Thermodynamics. *Anim. Feed Sci. Technol.* **2010**, *160*, 1–22. [[CrossRef](#)]
33. Rath, S.; Heidrich, B.; Pieper, D.H.; Vital, M. Uncovering the Trimethylamine-Producing Bacteria of the Human Gut Microbiota. *Microbiome* **2017**, *5*, 1–14. [[CrossRef](#)]
34. Guerra, C.A.; Heintz-Buschart, A.; Sikorski, J.; Chatzinotas, A.; Guerrero-Ramírez, N.; Cesarz, S.; Beaumelle, L.; Rillig, M.C.; Maestre, F.T.; Delgado-Baquerizo, M.; et al. Blind Spots in Global Soil Biodiversity and Ecosystem Function Research. *Nat. Commun.* **2020**, *11*, 1–13. [[CrossRef](#)] [[PubMed](#)]
35. Clarke, S.F.; Murphy, E.F.; O’Sullivan, O.; Lucey, A.J.; Humphreys, M.; Hogan, A.; Hayes, P.; O’Reilly, M.; Jeffery, I.B.; Wood-Martin, R.; et al. Exercise and Associated Dietary Extremes Impact on Gut Microbial Diversity. *Gut* **2014**, *63*, 1913–1920. [[CrossRef](#)]
36. Bodkin, D.; Cai, C.L.; Manlapaz-Mann, A.; Mustafa, G.; Aranda, J.V.; Beharry, K.D. Neonatal Intermittent Hypoxia, Fish Oil, and/or Antioxidant Supplementation on Gut Microbiota in Neonatal Rats. *Pediatr. Res.* **2022**, *92*, 109–117. [[CrossRef](#)]
37. Ewees, M.G.; Messiha, B.A.S.; Abo-Saif, A.A.; Abd El, H.A.E.-T. Is Coenzyme Q10 Effective in Protection against Ulcerative Colitis? An Experimental Study in Rats. *Biol. Pharm. Bull.* **2016**, *39*, 1159–1166. [[CrossRef](#)]
38. Gumbmann, M.R.; Williams, S.N. The Quantitative Collection and Determination of Hydrogen Gas from the Rat and Factors Affecting Its Production. *Proc. Soc. Exp. Biol. Med.* **1971**, *137*, 1171–1175. [[CrossRef](#)]
39. Strohl, K.P.; Thomas, A.J.; Jean, P.S.; Schlenker, E.H.; Koletsky, R.J.; Schork, N.J. Ventilation and Metabolism among Rat Strains. *J. Appl. Physiol.* **1997**, *82*, 317–323. [[CrossRef](#)]
40. Snytnikova, O.A.; Khlichkina, A.A.; Sagdeev, R.Z.; Tsentlovich, Y.P. Evaluation of Sample Preparation Protocols for Quantitative NMR-Based Metabolomics. *Metabolomics* **2019**, *15*, 1–9. [[CrossRef](#)]
41. Wishart, D.S.; Guo, A.; Oler, E.; Wang, F.; Anjum, A.; Peters, H.; Dizon, R.; Sayeeda, Z.; Tian, S.; Lee, B.L. HMDB 5.0: The Human Metabolome Database for 2022. *Nucleic Acids Res.* **2022**, *50*, D622–D631. Available online: <http://www.hmdb.ca> (accessed on 21 October 2022). [[CrossRef](#)] [[PubMed](#)]
42. Toshchakov, S.V.; Izotova, A.O.; Vinogradova, E.N.; Kachmazov, G.S.; Tuaeava, A.Y.; Abaev, V.T.; Evteeva, M.A.; Gunitseva, N.M.; Korzhenkov, A.A.; Elcheninov, A.G. Culture-Independent Survey of Thermophilic Microbial Communities of the North Caucasus. *Biology* **2021**, *10*, 1352. [[CrossRef](#)] [[PubMed](#)]
43. Hugerth, L.W. DegePrime, a program for degenerate primer design for broad-taxonomic-range PCR in microbial ecology studies. *Appl. Environ. Microbiol.* **2014**, *80*, 5116–5123. [[CrossRef](#)] [[PubMed](#)]
44. Merkel, A.Y. Analysis of 16S rRNA Primer Systems for Profiling of Thermophilic Microbial Communities. *Microbiology* **2019**, *88*, 671–680. [[CrossRef](#)]
45. Renaud, G.; Stenzel, U.; Maricic, T.; Wiebe, V.; Kelso, J. DeML: Robust Demultiplexing of Illumina Sequences Using a Likelihood-Based Approach. *Bioinformatics* **2015**, *31*, 770–772. [[CrossRef](#)]
46. Callahan, B.J.; McMurdie, P.J.; Rosen, M.J.; Han, A.W.; Johnson, A.J.A.; Holmes, S.P. DADA2: High-Resolution Sample Inference from Illumina Amplicon Data. *Nat. Methods* **2016**, *13*, 581–583. Available online: <https://benjjneb.github.io/dada2/tutorial.html> (accessed on 5 October 2022). [[CrossRef](#)]
47. Quast, C.; Pruesse, E.; Yilmaz, P.; Gerken, J.; Schweer, T.; Yarza, P.; Peplies, J.; Glöckner, F.O. The SILVA Ribosomal RNA Gene Database Project: Improved Data Processing and Web-Based Tools. *Nucleic Acids Res.* **2013**, *41*, 590–596. [[CrossRef](#)]
48. McMurdie, P.J.; Holmes, S. Phyloseq: An R Package for Reproducible Interactive Analysis and Graphics of Microbiome Census Data. *PLoS ONE* **2013**, *8*, e61217. [[CrossRef](#)]
49. Dixon, P. VEGAN, a Package of R Functions for Community Ecology. *J. Veg. Sci.* **2003**, *14*, 927–930. [[CrossRef](#)]
50. Lin, H.; Peddada, S.D. Analysis of Compositions of Microbiomes with Bias Correction. *Nat. Commun.* **2020**, *11*, 3514. [[CrossRef](#)]

51. Love, M.I.; Huber, W.; Anders, S. Moderated Estimation of Fold Change and Dispersion for RNA-Seq Data with DESeq2. *Genome Biol.* **2014**, *15*, 1–21. [[CrossRef](#)]
52. Liu, C.; Cui, Y.; Li, X.; Yao, M. Microeco: An R Package for Data Mining in Microbial Community Ecology. *FEMS Microbiol. Ecol.* **2021**, *97*, fiae255. [[CrossRef](#)]

**Disclaimer/Publisher’s Note:** The statements, opinions and data contained in all publications are solely those of the individual author(s) and contributor(s) and not of MDPI and/or the editor(s). MDPI and/or the editor(s) disclaim responsibility for any injury to people or property resulting from any ideas, methods, instructions or products referred to in the content.